electronic reprint

Acta Crystallographica Section B
Structural Science
ISSN 0108-7681

Refinement of framework disorder in dehydrated CaA zeolite from single-crystal synchrotron data

Florence Porcher, Mohamed Souhassou, Heinz Graafsma, Anna Puig-Molina, Yves Dusausoy and Claude Lecomte

Acta Crystallographica Section B
Structural Science
ISSN 0108-7681

Refinement of framework disorder in dehydrated CaA zeolite from single-crystal synchrotron data

Florence Porcher,[a]* Mohamed Souhassou,[a] Heinz Graafsma,[b] Anna Puig-Molina,[b] Yves Dusausoy[a] and Claude Lecomte[a]

[a]Laboratoire de Cristallographie et Modélisation des Matériaux Minéraux et Biologiques associé au CNRS, UPRESA 7036, Université Henri Poincaré Nancy I, BP 239, 54506 Vandœuvre-lès-Nancy CEDEX, France, and [b]European Radiation Synchrotron Facility, BP 220, 38043 Grenoble CEDEX, France

Correspondence e-mail: porcher@lcm3b.u-nancy.fr

Received 23 November 1999
Accepted 5 May 2000

An accurate knowledge of zeolite structure is required for understanding their selective sorption capacities and their catalytic properties. In particular, the positions of the exchangeable cations and their interactions with the framework are essential. The present study deals with the accurate crystal structure determination of a fully exchanged and fully dehydrated CaA zeolite ($Ca_{48}Al_{96}Si_{96}O_{384}$, $Fm\bar{3}c$, $a = 24.47$ Å) using single-crystal high-resolution synchrotron X-ray diffraction [$(\sin\theta/\lambda)_{max} = 1.4$ Å^{-1}]. It is shown that cation exchange severely distorts the skeleton, especially around the O2 atom. The high-resolution synchrotron data reveal that this latter O atom is disordered and lies out of the mirror plane it occupies in other A-type zeolites. This feature is related to that observed for Ca^{2+} cations.

1. Introduction

Zeolite A, an aluminosilicate from the tectosilicate group, possesses a framework formed by a cubic array of cuboctahedral sodalite cages of 12 SiO_4 and AlO_4 corner-sharing tetrahedra. The alternation of the tetrahedra in the structure, in agreement with Löwenstein's rule (Löwenstein, 1954) for a Si/Al ratio of unity assessed by NMR (Lipmaa *et al.*, 1981), is responsible for a doubling of the cubic unit cell from $a \simeq 12$ Å (space group $Pm\bar{3}m$) to $a \simeq 24$ Å (space group $Fm\bar{3}c$) and for the existence of weak substructure reflections hkl ($h, k, l = 2n + 1$). The formal -1 charge borne by each AlO_4 is balanced by exchangeable cations lying in three types of sites in the cavities (Fig. 1), which influence the sorption properties of these materials. The crystal structure of dehydrated zeolite CaA has been studied over the last 20 years by single-crystal X-ray diffraction (Firor & Seff, 1978; Pluth & Smith, 1983) and powder neutron diffraction (Adams & Haselden, 1984), but these studies disagree on the location of Ca^{2+} cations in the voids. Moreover, the displacement ellipsoids of the O2 atom appear to be very elongated in all three structure determinations, suggesting a positional disorder of this atom that cannot be resolved from low-resolution data. Our aim is to determine the electron density and related electrostatic properties of various zeolites in order to understand their sorption properties. In the case of the CaA zeolite, it is first needed to locate the charge-compensating cations and to precisely determine the crystal structure.

2. Experimental

2.1. Sample preparation and characterization

Single crystals of NaA zeolite were prepared by a modified Charnell's method (Charnell, 1971) without seeding. Ion

exchange was performed by a flow method, a continuous stream of fresh solution of $CaCl_2$ flowed through the crystals over 26 h with an approximate flux of 50 ml h^{-1}. The molarity of the solution was 1.5 and its pH was 7. Afterwards, the solution was drained and crystals were carefully rinsed with 500 ml of distilled water and dried. Microprobe analysis showed no residual sodium in the crystals. Colorless and transparent single crystals were selected and mounted in thin quartz capillaries with approximate diameter 150 µm. These capillaries and a control NMR tube were progressively heated up to 723 K for 6 d under a vacuum of 3.10^{-9} bars, then sealed at room temperature under vacuum (Porcher, 1998; Porcher *et al.*, 1999). Optical examination showed that the crystals remained colorless and transparent. The ^{1}H NMR analysis showed no signal indicating for residual water (less than 0.03 wt%) and the ^{27}Al NMR (Fyfe *et al.*, 1982) spectrum did not exhibit any characteristic signal of octahedrally coordinated aluminium, attesting the preservation of the framework during dehydration.

2.2. Data collection

The diffraction intensities were measured at room temperature with synchrotron radiation (λ = 0.248 Å) at the material science beamline ID11 of the ESRF. Measurement was performed on a diffractometer with a CCD detector [Siemens (Brücker) Smart CCD system]. Frames were indexed, integrated and scaled using *SMART* and *SAINT* software packages (Siemens, 1995) without including the extinction conditions of a (110) *c* glide mirror. Owing to the short wavelength (0.248 Å), no absorption correction was applied (µ = 0.074 mm^{-1}). In order to assess the symmetry of the crystal, the 16 629 measured reflections were merged without rejection (*SORTAV*, Blessing, 1989) in two Laue groups: $m\bar{3}m$, which allows the centrosymmetric space group $Fm\bar{3}c$ and the noncentrosymmetric space groups $F4\bar{3}c$ and $F432$, and $m\bar{3}$, corresponding to $Fm\bar{3}$ and $F23$. Despite a redundancy 1.5 times greater in $m\bar{3}m$ than in $m\bar{3}$, the internal agreement factors R and wR are equal (Table 1), therefore, the $m\bar{3}m$ symmetry was retained for further analysis. Only 10 reflections violating the *c* glide mirror were observed, all being measured only once. Four of them had $I > 3\sigma(I)$, the strongest being 41, 41, 25, $I/\sigma(I) = 4.5$, suggesting some indexing problem or bad evaluation of the weak reflections; the assessment of systematic absence therefore discards the $F432$ space group. The two possible remaining space groups, $F\bar{4}3c$ and $Fm\bar{3}c$, were tested during the structure refinements after the rejection of statistical outliers in the intensity distribution of symmetry-equivalent reflections (Table 1).

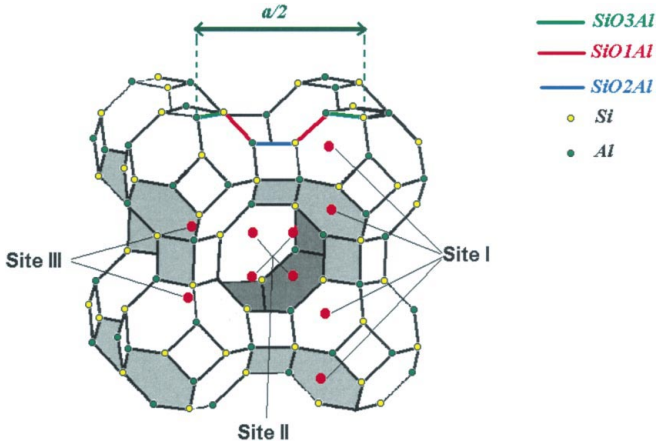

Figure 1
A Si–Al representation of the framework of zeolite A with cation sites.

Table 1
Intensity measurements and data reduction parameters.

Statistical agreement for structure refinement with hypothesis *a*, *b*, *c* and *d*	
Dehydrated CaA zeolite ($Fm\bar{3}c$)	
Composition per unit cell ($Z = 1$)	$Ca_{48}Al_{96}Si_{96}O_{384}$
Space group	$Fm\bar{3}c$
Cell parameter (Å); volume (Å^3); calculated density (g cm^{-3})	24.47 (1); 14 652 (18); 1.52
Temperature (K); exposure time (h)	293; 8
Radiation	ESRF; λ = 0.248 Å
Crystal shape, size	Cube {100}, 90 µm along [1,0,0]
Absorption coefficient (cm^{-1})	µ = 0.74
Reflections measured; $(\sin\theta/\lambda)_{max}$ (Å^{-1})	16 629; 1.4

	Internal agreement factors before any rejection		Internal agreement factors after rejection of statistical outliers	
	R	*wR*	*R*	*wR*
$m\bar{3}m$	0.064	0.037	0.059	0.037
$m\bar{3}$	0.063	0.035		

Unique reflections	1269 from which 245 of substructure
Reflections used in least-squares refinement ($I > 0\sigma$)	1147 from which 222 of substructure
Reflections set reserved for R_{free}	122 from which 23 of substructure

Statistical agreement at the end of least-squares refinements 1147 reflections with $I > 0\sigma(I)$ and $0 < (\sin\theta/\lambda) < 1.4$ Å^{-1}

	Hypothesis *a*	Hypothesis *b*	Hypothesis *c*	Hypothesis *d*
$R(F)$	0.077	0.070	0.066	0.068
$wR(F)$	0.074	0.067	0.062	0.064
$R_{free}(F)$	0.077	0.072	0.067	0.074
$wR_{free}(F)$	0.084	0.077	0.069	0.073

2.3. Structure determination and refinement in $Fm\bar{3}c$

The crystal structure was redetermined by direct methods using the *NRCVAX* program package (Gabe *et al.*, 1989) with neutral atom scattering factors. A subset of ∼10% of the reflections (122 out of 1269) was reserved and not used in the least-squares refinements in order to validate the successive structural hypothesis (R_{free} factor; Brünger, 1992). All other 1147 reflections with $I > 0$ were used for the refinements, but Fourier syntheses were calculated using structure factors with $I > 3\sigma(\sigma)$. After location of the framework atoms [$R(F) = 0.23$, $wR(F) = 0.31$, 1147 reflections, $R_{free}(F) = 0.23$, $wR_{free}(F) = 0.31$], difference Fourier maps along the threefold axis (Fig. 2) showed an elongated density peak with three maxima at

(0.061, 0.061, 0.061), (0.086, 0.086, 0.086) and (0.104, 0.104, 0.104) of respective heights 7.5, 13.0 and 13.5 e Å^{-3}. These peaks were introduced subsequently in the refinement as calcium atoms Ca1, Ca2 and Ca3 with respective occupancy factors of 15, 30 and 30% according to their height and to the expected chemical formula [$R(F)$ = 0.081, $wR(F)$ = 0.078]. Difference Fourier maps calculated at this stage revealed that the electron density peaks at Ca1 and Ca2 positions were correctly modeled, but three peaks located around Ca3 (Fig. 3) remained, suggesting further positional disorder. This disorder was modeled by splitting the Ca3 site in three sites, related by the threefold symmetry and with a fixed occupancy factor of 10%. This splitting reduced the statistical agreement to $R(F)$ = 0.077 and $wR(F)$ = 0.074, removing the three previously observed electron density peaks (Fig. 8, see supplementary materials[1]). At this stage (hypothesis *a*), the atomic displacement ellipsoid of the O2 atom was very elongated along the [100] direction (CIF available as deposited material), with electron density residues at each side of the atom position. Our high-resolution data (d_{min} = 0.36 Å, $\sin\theta/\lambda_{max}$ = 1.4 Å^{-1}) allowed us to resolve the positional disorder of this atom. The high-resolution Fourier synthesis map at the O2 position (Fig. 4) clearly showed two maxima at [± 0.27 (3) Å] above and below the mirror plane (0*yz*), where the O2 atom was constrained to sit. After splitting this O2 atom site into two components with 50% occupancies (hypothesis *b*), atomic displacement parameters of O2 became almost isotropic with U^{11} decreasing from 0.130 (4) to 0.031 (2) Å^2. Electron density peaks around the mean position of O2 disappeared and agreement factors reduced significantly [$R(F)$ = 0.0699 and $wR(F)$ = 0.0672]. Free *R* indices (calculated with the 122 reflections reserved) also decreased smoothly (see Table 1), being slightly higher than *R* and *wR* factors for all refinement steps and thus validating the successive introductions of cations and the disordered model for O2. Structural parameters at this step of refinement (hypothesis *b*) are given in Table 2.

At this stage of refinement, a peak of 6.1 e Å^{-3} remained at the high symmetry position (0, 0, 0) ($m\bar{3}$), see Fig. 5. Despite the absence of chemically realistic coordination for a Ca^{2+} cation on this site, a calcium atom Ca4 was introduced with various occupancies and its isotropic atomic displacement parameter refined. For high fixed occupancy values (> 0.125), thermal displacement parameters became very large and both *R* and R_{free} increased. Therefore, the occupation factor should be rather small. Starting with an occupancy factor of 0.125, subsequent joint refinement of occupancies and thermal displacement parameters of all cations converged to a final occupancy of 0.088 (1) for Ca4 [U_{iso} = 0.03 (1) Å^2, $R(F)$ = 0.0660 and $wR(F)$ = 0.0623]. This hypothesis (hypothesis *c*) leads to 16 (1) Ca1, 11 (1) Ca2, 23.8 (6) Ca3 and 0.64 (8) Ca4 cations, and to a total of 51.4 (30) Ca^{2+} cations per unit cell [50.8 (30) without Ca4] in good agreement with the value (48) predicted on an electroneutrality basis. Structural parameters at the end of this refinement are available in the CIF, deposited.

Table 2
Fractional atomic coordinates and equivalent isotropic displacement parameters (Å^2).

$$U_{eq} = (1/3)\Sigma_i\Sigma_j U^{ij} a^i a^j \mathbf{a}_i.\mathbf{a}_j.$$

	Occupancy	*x*	*y*	*z*	U_{eq}
Si		0	0.09216 (6)	0.18413 (5)	0.01648 (5)
Al		0	0.18738 (5)	0.09095 (6)	0.0180 (6)
O1		0	0.1088 (1)	0.2460 (2)	0.047 (2)
O2	0.5	0.0115 (1)	0.1423 (2)	0.1436 (2)	0.031 (3)
O3		0.0539 (1)	0.0577 (1)	0.1676 (1)	0.045 (2)
Ca1	0.15	0.0685 (1)	0.0685 (1)	0.0685 (1)	0.040 (2)
Ca2	0.3	0.0874 (2)	0.0874 (2)	0.0874 (2)	0.0446 (1)
Ca3	0.1	0.1052 (9)	0.0977 (2)	0.1090 (9)	0.023 (4)

Ca4 refinement reduced the height of the electron density peak at (0, 0, 0) from 6.1 to 1.4 e Å^{-3}. Correlatively, both *R* and R_{free} factors decreased by 0.005 (see Table 3), especially in the lower resolution shells with $\sin\theta/\lambda < 0.6$ Å^{-1}. Therefore, an hypothesis with an atom at (0, 0, 0) cannot be rejected. However, all neighboring O atoms are at more than 4.5 Å from the (0, 0, 0) position and cannot interact strongly with any atom sitting there. Also, one has to bear in mind that this site has a high symmetry ($m\bar{3}$, site symmetry 24), so the estimated standard uncertainty on electron density in such a position reaches at least 0.5 e Å^{-3}.

We have to note that for refinement (*c*) the GOF is larger that the expected value of one, the weighting scheme used being $w = (\sigma^2)^{-1}$. This is partly due to the underestimation of the standard uncertainties of the strong reflections by the *SAINT* program (Siemens, 1995), as already pointed out in one of our previous papers (Kuntzinger *et al.*, 1999).

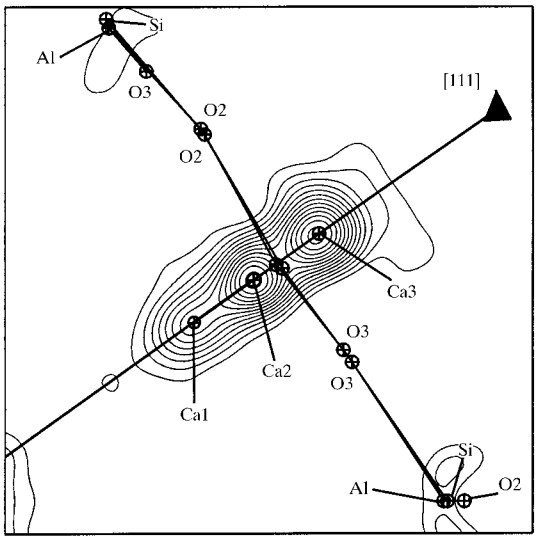

Figure 2
Difference Fourier map showing electron density peaks along the threefold axis at the position of the Ca atoms (contours 1.0 e Å^{-3}).

[1] Supplementary data for this paper are available from the IUCr electronic archives (Reference: BR0095). Services for accessing these data are described at the back of the journal.

Table 3
Statistical agreement as a function of resolution shell for hypotheses *b* and *c*.

Statistical agreement after least-squares refinements sin θ/λ = 1.4 Å^{-1}											
		Hypothesis *b*: site (0, 0, 0) empty					Hypothesis *c*: Ca4 at site (0, 0, 0)				
sin $(\theta/\lambda)_{min}$ (Å^{-1})	No. of reflections	*R*	*wR*	R_{free}	wR_{free}	ρ_{max} at (0, 0, 0) (e Å^{-3})	*R*	*wR*	R_{free}	wR_{free}	ρ_{max} at (0, 0, 0) (e Å^{-3})
0.0	1147	0.070	0.067	0.072	0.077	6.1	0.066	0.062	0.067	0.069	1.4
0.4	1011	0.077	0.063	0.082	0.070	4.2	0.075	0.060	0.080	0.065	0.8
0.6	742	0.097	0.076	0.099	0.086	2.4	0.096	0.075	0.098	0.084	0.6
0.8	346	0.142	0.124	0.122	0.097	1.2	0.142	0.125	0.117	0.096	0.7

Furthermore, as shown on the $\Delta\rho$ residual density map, there are still features (*ca* $\pm$1.5 e Å^{-3}), which are not taken into account by the refinement model, contributing to the high GOF.

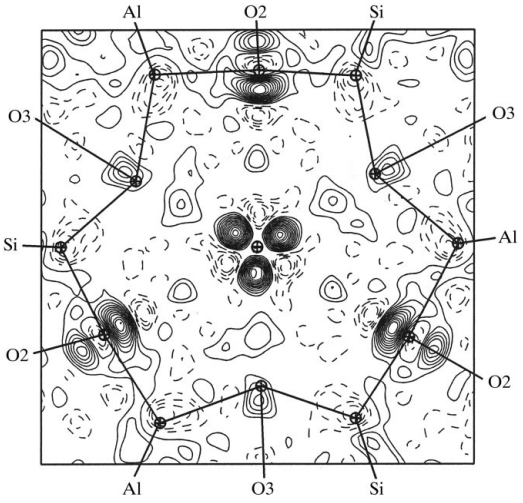

Figure 3
Difference Fourier map in a plane perpendicular to the threefold axis showing electron density peaks owing to a disorder of Ca3 (contours 0.1 e Å^{-3}).

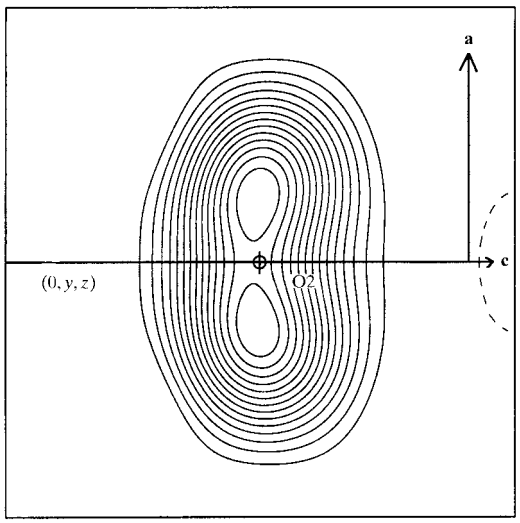

Figure 4
Fourier synthesis map at the O2 position (contours 1.0 e Å^{-3}).

2.4. Structure determination and refinement in $F\bar{4}3c$

The crystal structure of CaA was also independently solved again in space group $F\bar{4}32$ (hypothesis *d*). In this space group the Si, Al and O1 atoms that sit in the mirror plane perpendicular to [100] in the space group $Fm\bar{3}c$ were allowed to move out of this plane. Other atom sites (O2, O3), which are generated twice by the mirror plane perpendicular to [100] in $Fm\bar{3}c$, were split into two components with partial occupancies summing 1 when refining the structure in $F\bar{4}3c$. The position of calcium ions were found from difference Fourier maps. The determination of the structure led to cation positions in agreement with those found in $Fm\bar{3}c$. The O2 atom was found to be disordered in the same fashion as in $Fm\bar{3}c$ and the residue at (0, 0, 0) had a similar height. Unexpectedly, all the correlations between former mirror symmetry-related atomic parameters remained low (0.7–0.8) during structural refinements, but statistical indices were not improved [$R(F)$ = 0.0700, $wR(F)$ = 0.0667]. Comparison of structural parameters at the end of the refinement with those obtained in $Fm\bar{3}c$ (see CIF, deposited) showed that departure of Si, Al, O1 atoms from the (100) mirror symmetry was not significant, with differences between *m* symmetry-related parameters less than four times their estimated standard uncertainties. As a consequence, space group $Fm\bar{3}c$ is statistically more significant than $F\bar{4}3c$. Bond lengths and angles of hypothesis *b*, which represents the most likely structure, are given in Table 4.

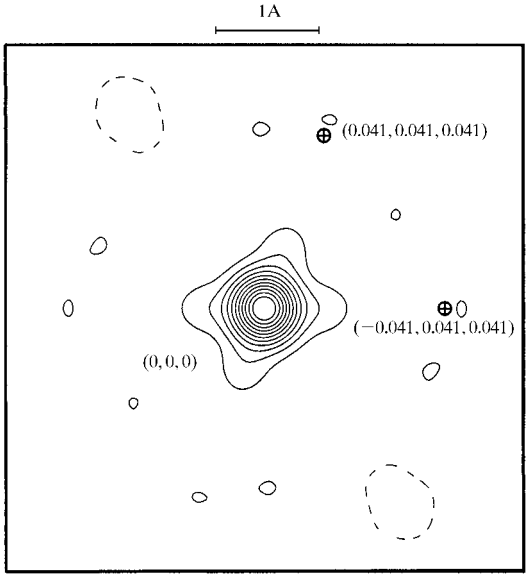

Figure 5
Difference Fourier map in the plane containing (0, 0, 0), (0.041, 0.041, 0.041) and (−0.041, 0.041, 0.041), showing the electron density residue at the Ca4 position (hypothesis *b*; contours 0.5 e Å^{-3}).

Table 4
Bond lengths (Å) and bond angles (°) of the framework and coordination distances of Ca^{2+} cations in dehydrated CaA zeolite (hypotheses *a* and *b*).

Refinement 1 (hypothesis *a*)						Refinement 2 (hypothesis *b*)					
Framework geometry											
Si—O1	1.568 (5)	Al—O1	1.687 (5)			Si—O1	1.568 (5)	Al—O1	1.688 (5)		
Si—O2	1.577 (3)	Al—O2	1.697 (4)			Si—O2	1.603 (5)	Al—O2	1.719 (5)		
Si—O3	1.611 (2)	Al—O3	1.745 (2)			Si—O3	1.617 (3)	Al—O3	1.746 (3)		
O1—Si—O2	114.0 (2)	O1—Al—O2	115.7 (2)			O1—Si—O2	113.5 (2)	O1—Al—O2	115.2 (2)		
O1—Si—O3	112.1 (1)	O1—Al—O3	113.7 (1)			O1—Si—O3	112.2 (1)	O1—Al—O3	113.7 (1)		
O2—Si—O3	104.7 (1)	O2—Al—O3	102.6 (1)			O2—Si—O3	95.8 (2)	O2—Al—O3	110.1 (2)		
O3—Si—O3	108.7 (1)	O3—Al—O3	107.3 (1)			O2—Si—O3	112.8 (2)	O2—Al—O3	94.5 (2)		
						O3—Si—O3	109.3 (2)	O3—Al—O3	107.9 (1)		
Si—O1—Al	149.9 (3)	Si—O2—Al	169.8 (3)	Si—O3—Al	141.6 (2)	Si—O1—Al	150.0 (2)	Si—O2—Al	157.9 (2)	Si—O3—Al	140.9 (2)
Coordination of cations											
Ca1—O3	2.476 (8)	Ca2—O3	2.260 (2)	Ca3—O3	2.15 (4)	Ca1—O3	2.465 (3)	Ca2—O3	2.248 (5)	Ca3—O3	2.14 (2)
				Ca3—O3	2.26 (4)					Ca3—O3	2.25 (2)
				Ca3—O3	2.48 (4)					Ca3—O3	2.47 (2)

3. Discussion

3.1. Location of Ca^{2+} cations in dehydrated CaA

3.1.1. Comparison with earlier structural studies. The most probable hypothesis is that Ca^{2+} cations lie on three types of sites of type I, on or around the threefold axis near a hexagonal window of a sodalite cage. Ca1, like Ca2, is coordinated to three O3 atoms with respective coordination distances of 2.465 (3) and 2.248 (5) Å. Ca3 has a distorted coordination polyhedron with two unusually short bonds [2.14 (2) and 2.25 (2) Å] with O3 atoms and two longer bonds with O2 [2.47 (3) Å]. Relative occupancies of the three sites agree with mean coordination distances, site I(*a*) at (0.0685, 0.0685, 0.0685), which exhibits longer mean coordination distances, being less occupied than site I(*b*) (0.0874, 0.0874, 0.0874) and the threefold related sites I(*c*) (0.1052, 0.0977, 0.1090).

In all four structural studies described in Table 5 (including this work), site I is occupied and split, but the subsite occupancies differ totally. Site II, in the eight-membered window joining two α-cages, is only occupied in the structure of Firor & Seff (1978). Its position, similar to that of sodium cations in NaA zeolite, might indicate an incomplete cation exchange. A residual was found in site IV (0, 0, 0), whose electron density was refined as a Ca atom (0.6 atoms per unit cell). As this site is far from all O atoms, such an atom cannot be chemically justified; also the chemical nature of this residue is very uncertain and cannot be assessed even on the basis of our very accurate measurements. One has to notice that Pluth & Smith (1983) have found an electron density peak at (0, 0, 0) (site IV) linked to neighboring peaks at (0.041, 0.041, 0.041) attributed to an AlO_2H complex supposely formed during cation exchange. Since no electron density peaks at (0.041, 0.041, 0.041) are present in our electron density map (Fig. 9, see supplementary material), this hypothesis has been discarded for our crystal.

3.1.2. Comparison of the location of cations in various dehydrated A-type zeolites. The crystal structures of LiA (Porcher *et al.*, 1998), NaA (Pluth & Smith, 1980; Porcher, 1998), KA (Pluth & Smith, 1979), SrA (Pluth & Smith, 1982) and TlA (Cheetham *et al.*, 1982) show that the 96 monovalent cations are mainly distributed on two sites: site I, on the threefold axis and near a six-membered ring, and site II on or near the (100) mirror plane in the eight-membered window. Site I, which may be split in the case of divalent cations, is almost fully occupied. The two types of sites II, respectively corresponding to a cation position close to O1 (NaA, KA, TlA) or O2 (LiA), have a partial occupancy close to 0.25, corresponding to a mean occupation of each window by one cation. Site III at (0.25, 0.1, 0.1) shows no coordination with O atoms and has been found to be empty in recent studies (Papoular & Cox, 1995; Porcher, 1998). Higher occupancy for site I than for site II indicates that the former site is energetically more favorable, in agreement with a better coordination to O atoms. When the charge compensating cations are

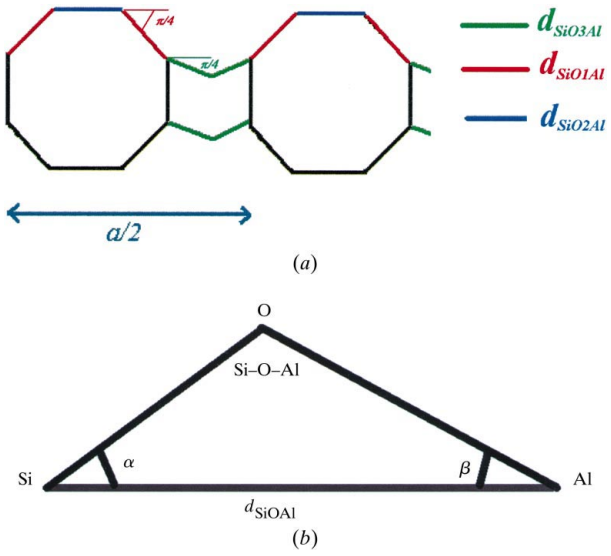

Figure 6
Three-dimensional scheme illustrating the calculation of cell parameters according to equation (1) as a function of Si—Al distances (Å) through O1, O2 and O3 atoms. The color scheme for Si—Al bridges is the same as for Fig. 1.

Table 5
Cation sites in dehydrated CaA from different studies.

	$Ca_{48}Si_{96}Al_{96}O_{384}$ [(a)]	$Ca_{41.6}Na_{3.2}Si_{100}Al_{92}O_{384}$ [(b)]	$Ca_{40}Na_{16}Si_{96}Al_{96}O_{384}$ [(c)]	$Ca_{48}Si_{96}Al_{96}O_{384}$ [(d)]
Space group	$Pm\bar{3}m$	$Fm\bar{3}c$	$Fm\bar{3}c$	$Fm\bar{3}c$
Site I occupancy	(0.079, 0.079, 0.079)	(0.079, 0.079, 0.079)		(0.068, 0.068, 0.068)
	0.125	0.153		0.15
	(0.095, 0.095, 0.095)		(0.089, 0.089, 0.089)	(0.087, 0.087, 0.087)
	0.125		0.625	0.30
	(0.106, 0.106, 0.106)	(0.103, 0.103, 0.103)	(0.109, 0.109, 0.109)	(0.105, 0.098, 0.109)
	0.375	0.544	0.25	0.10†
Site II occupancy	(0, 0.234, 0.234)			
	0.083			
Site IV occupancy		Al (0, 0, 0)		
		0.35		
		O (0.041, 0.041, 0.041)		
		0.15		

References: (*a*) Firor & Seff (1978); (*b*) Pluth & Smith (1983); (*c*) Adams & Haselden (1984); (*d*) this work (hypothesis *b*). † The comparable value of occupancy for a cation sitting on a threefold axis is 0.30.

Table 6
Cell parameters (Å) and framework geometries of various A-type zeolites.

	LiA[(a)]	NaA[(b)]	KA[(c)]	TlA[(d)]	SrA[(e)]	CaA	CaA Hypothesis *b*
Cell parameter	23.90	24.56	24.60	24.373	24.68	24.47	24.47
Si—O1—Al	173.7 (3)	145.2 (4)	128.5 (3)	150.5	141.3 (2)	149.9 (2)	150.0 (2)
Si—O2—Al	133.0 (2)	159.7 (4)	177.2 (3)	149.7	177.5 (3)	169.8 (3)	157.9 (2)
Si—O3—Al	129.5 (1)	143.1 (3)	151.9 (2)	140.4	146.8 (2)	141.6 (2)	140.9 (2)
⟨Si—O—Al⟩†	141.4	149.1	152.4	145.3	153.1	150.8	147.4
O1—Si—O2	109.1 (2)	107.9 (5)	108.0 (3)	104.9	113.8 (2)	114.0 (2)	113.5 (2)
O1—Si—O3	111.2 (1)	111.3 (4)	110.8 (2)	110.5	111.6 (1)	112.1 (1)	112.2 (1)
O2—Si—O3	108.6 (2)	107.7 (4)	108.0 (2)	108.7	104.9 (1)	104.7 (1)	95.8 (2)
							112.8 (2)
O3—Si—O3	108.2 (2)	110.6 (5)	111.1 (3)	113.2	109.7 (2)	108.7 (1)	109.3 (2)
O1—Al—O2	107.6 (2)	106.8 (4)	107.7 (3)	105.4	114.2 (3)	115.7 (2)	115.2 (2)
O1—Al—O3	112.8 (1)	112.4 (5)	111.2 (2)	111.7	111.6 (2)	113.7 (1)	113.7 (1)
O2—Al—O3	107.0 (2)	106.6 (5)	106.9 (2)	107.5	105.0 (2)	102.6 (1)	94.5 (2)
							110.1 (2)
O3—Al—O3	109.3 (2)	110.2 (5)	112.6 (3)	112.5	109.2 (3)	107.3 (1)	107.9 (1)

References: (*a*) Porcher *et al.* (1998); (*b*) Porcher (1998); (*c*) Pluth & Smith (1979); (*d*) Cheetham *et al.* (1982); (*e*) Pluth & Smith (1982). † ⟨Si—O—Al⟩ is the average angle [(Si—O1—Al) + (Si—O2—Al) + 2(Si—O3—Al)]/4 weighted by the relative number of O atoms according to their site symmetry.

divalent, site I has a high enough multiplicity to accommodate all 48 cations and site II is not occupied. This is also shown in the structural studies of CaA and SrA (Firor & Seff, 1978; Pluth & Smith, 1982).

3.2. Framework distortion with cation exchange

The variation of the cell parameter with the nature of the charge compensating cation M is important for zeolites $M-A$ and $M-X$, particularly for $Na^+ \rightarrow Li^+$ exchange (Table 6). It is due to a conformational adaptation of the nonrigid framework in order to optimize the coordination of cations with various charges and ionic radii. This deformation is almost totally absorbed by the Si—O—Al angles as confirmed by Table 6, which shows that while SiO_4 and AlO_4 tetrahedra act as rigid entities with only slight variation of O—T—O angles of a few degrees, the angular variation in Si—O—Al can be substantial. One can note that while the mean value of $\langle Si-O-Al\rangle_{M-A}$ is similar for KA, NaA, CaA and TlA ($150 \pm 5^\circ$), the angular dispersion around the mean for a given Si—O—Al angle (Si—O1—Al or Si—O2—Al or Si—O3—Al) can reach 30° (LiA).

For zeolites A, the geometry of the structure is simple enough to give an estimate of the cell parameter as a function of the silicon to aluminium distance. Fig. 1 is the usual Si–Al representation of the framework of zeolite A, where the Si–Al segments are differentiated as a function of the bridging O atom. Fig. 6(*a*) in the (0, *y*, *z*) mirror plane shows that the cell parameter *a* can be calculated easily knowing the Si—Al distances d_{SiO1Al}, d_{SiO2Al} and d_{SiO3Al} through oxygen atoms O1, O2 and O3

$$a = 2\left[d_{SiO1Al} + 2d_{SiO2Al} * \cos(\pi/4) + 2d_{SiO3Al} * \cos(\pi/4)\right]. \quad (1)$$

If one assumes that the tetrahedra really act as rigid entities and are kept undistorted in all structures and that the O2 atom only depart slightly from the (100) mirror plane, it is possible to simplify a further previous expression assigning to all Si—O and Al—O distances their mean values of 1.60 and 1.73 Å. Each d_{SiOAl} distance becomes (Fig. 6*b*)

$$d_{SiOAl} = \langle SiO\rangle * \cos\alpha + \langle AlO\rangle * \cos\beta. \quad (2)$$

Since

$$\beta = \pi - \alpha - SiOAl \quad \text{and}$$
$$\beta = \arcsin[(\langle SiO\rangle/\langle AlO\rangle)\sin\alpha] \quad (3)$$

values for α can be iteratively found from Si—O—Al angles, the cell parameter then becomes a function of Si—O—Al angles. This expression of the cell parameter of zeolites A as a function of Si—O—Al angles can be used to test crystal structures, knowing experimental values of the cell para-

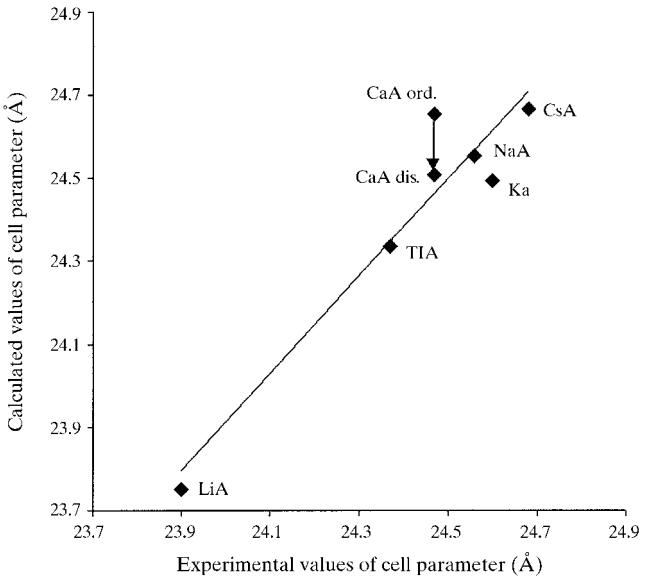

Figure 7
Calculated cell parameter (Å) of LiA, NaA, Ka, SrA and CaA (O2 ordered or disordered) as a function of observed values.

meters. Fig. 7 is the plot of calculated cell parameter values for dehydrated LiA, NaA, KA, CsA and CaA in ordered (hypothesis *a*) and disordered (hypothesis *b*) hypotheses as a function of experimental values. It shows that our simple model works fairly well for all zeolite types, except ordered CaA and KA. In the case of CaA, keeping O2 constrained to lie in the mirror plane (100) requires distortions of the framework, not only in the Si—O2—Al angle [169.8 (3)°], but also in Si—O and Al—O bond lengths; the calculated value of the cell parameter disagrees with the experimental one. The displacement of O2 out of the (100) plane ensures a relaxation of the CaA framework, with a diminution of the Si—O2—Al angle [157.9 (2)°] and a preservation of the tetrahedra, as assessed by the better agreement of calculated and observed values for the cell parameter.

4. Conclusions

The high resolution study on a single-crystal of dehydrated CaA zeolite has provided evidence of the structural disorder of Ca^{2+} cations which can be related to the disorder of the O2 atoms. The disorder of O2 explains the very high atomic displacement factors found in all the previous studies. Lowering the symmetry from $Fm\bar{3}c$ to $F\bar{4}3c$ led to similar conclusions and was statistically indistinguishable.

The authors thank the Air Liquide company who funded this project. They are grateful to Drs Caullet and Kessler, Ecole Nationale Supérieure de Chimie de Mulhouse, for their help in the zeolite-A syntheses, Dr A. Fonseca, Laboratoire de RMN de la faculté Universitaire Notre-Dame de la Paix (Namur, Belgium), for the NMR measurements, J. Reymann, J. L. Vasseur and J. P. Dècle (LCM^3B) for constructing and running the dehydration apparatus.

References

Adams, J. M. & Haselden, D. A. (1984). *J. Solid State Chem.* **51**, 83–90.
Blessing, R. H. (1989). *J. Appl. Cryst.* **22**, 396–397.
Brünger, A. T. (1992). *Nature*, **355**, 472–474.
Charnell, J. F. (1971). *J. Cryst. Growth*, **8**, 291–294.
Cheetham, A. K., Eddy, M. M., Jefferson, D. A. & Thomas, J. M. (1982). *Nature*, **299**, 24–26.
Firor, R. L. & Seff, K. (1978). *J. Am. Chem. Soc.* **100**, 3091–3096.
Fyfe, C. A., Gobbi, G. C., Hartman, J. S., Klinowski, J. & Thomas, J. M. (1982). *J. Phys. Chem.* **86**, 1247–1250.
Gabe, E. J., Lepage, Y., Charland, J. P., Lee, F. L. & White, P. S. (1989). *J. Appl. Cryst.* **22**, 384–387.
Kuntzinger, S., Dahaoui, S., Ghermani, N. E., Lecomte, C. & Howard, J. A. K. (1999). *Acta Cryst.* B**55**, 867–881.
Lipmaa, E., Mägi, M., Samoson, A., Tarmak, M. & Engelhardt, G. (1981). *J. Am. Chem. Soc.* **103**, 4992–4996.
Löwenstein, W. (1954). *Am. Mineral.* **39**, 92–96.
Papoular, R. J. & Cox, D. E. (1995). *Europhys. Lett.* **32**, 337–342.
Pluth, J. J. & Smith, J. V. (1979). *J. Phys. Chem.* **83**, 741–749.
Pluth, J. J. & Smith, J. V. (1980). *J. Am. Chem. Soc.* **102**, 4704–4708.
Pluth, J. J. & Smith, J. V. (1982). *J. Am. Chem. Soc.* **104**, 6977–6982.
Pluth, J. J. & Smith, J. V. (1983). *J. Am. Chem. Soc.* **105**, 1192–1195.
Porcher, F. (1998). Thèse de doctorat de l'Université Henri Poincaré – Nancy 1, France.
Porcher, F., Souhassou, M., Dusausoy, Y. & Lecomte, C. (1998). *C. R. Acad. Sci. Paris*, t. 1, Série IIc, 701–708.
Porcher, F., Souhassou, M., Dusausoy, Y. & Lecomte, C. (1999). *Eur. J. Mineral.* **11**, 333–343.
Siemens (1995). *Siemens Analytical X-ray Instruments Inc.* Madison, Wisconsin, USA.